Atomic oxygen species on silver: Photoelectron spectroscopy and x-ray absorption studies

V. I. Bukhtiyarov,[1,*] M. Hävecker,[2] V. V. Kaichev,[1] A. Knop-Gericke,[2] R. W. Mayer,[2] and R. Schlögl[2]
[1]*Boreskov Institute of Catalysis, Lavrentieva Avenue 5, 630090, Novosibirsk, Russia*
[2]*Fritz-Haber-Institut der MPG, Faradayweg 4-6, D-14195 Berlin (Dahlem), Germany*
(Received 9 April 2002; revised manuscript received 29 August 2002; published 27 June 2003)

Two oxygen species, which are constituents of the active centers for ethylene epoxidation over silver, have been characterized by a number of physical methods sensitive to adsorbate electronic structure such as x-ray photoelectron, ultraviolet photoelectron, Auger, and x-ray-absorption near-edge structure spectroscopy. One of the species denoted as nucleophilic oxygen due to its activity in total oxidation only exhibits spectroscopic characteristics close to those of bulk Ag_2O. This allows us to describe this species as atomically adsorbed oxygen in the structure of surface silver(I) oxide. The considerable extent of the covalency in bonding of this oxidelike oxygen with the silver surface due to hybridization of O2p levels with Ag4d and Ag5sp orbitals should be also emphasized. Contrary to this, only 5sp orbitals of silver hybridize with 2p orbitals of oxygen as the other oxygen species forms. As a consequence, this species being also atomic oxygen is characterized by a lower oxygen-silver bonding interaction and a lower charge on the oxygen. The latter causes the activity of this electrophilic species in epoxidation. Possible models of adsorption centers for these oxygen species are discussed.

DOI: 10.1103/PhysRevB.67.235422 PACS number(s): 73.20.At

I. INTRODUCTION

The well-known activity of silver as a catalyst for selective oxidation of a number of hydrocarbons (not only ethylene[1–4] or methanol,[5] but also styrene[6] and methane[7]) has generated during the last 30 years a huge number of investigations devoted to the interaction of oxygen with silver surfaces (see, for example, Refs. 4, and 8–20). Surface science has identified various oxygen species adsorbed on silver. It has been shown that at low temperatures, oxygen is adsorbed molecularly.[11–15] Heating causes dissociation of $O_{2,ads}$ and/or its desorption at 170–220 K, with both the temperature and the route of transformation being dependent on the surface structure of silver. Atomic oxygen is stable up to ~600 K when its associative desorption takes place.[8–17] Furthermore, at $T \geqslant 420$ K surface oxygen atoms can dissolve into the silver bulk.[10,11] This scheme of oxygen states and their mutual transformations has been summarized in a comprehensive review.[4]

At the same time, there are many experimental results, which indicate that the above-mentioned picture of oxygen states is oversimplified and that it would be more correct to identify three classes of states, each of which includes a few species with various electronic properties. For instance, Campbell and Paffett[13] have shown that both peroxide and superoxide[14,15] states of $O_{2,ads}$ are formed on the surfaces of single silver crystals. In the papers of van Santen *et al.*, it has been revealed experimentally[3,4] and theoretically[18] that dissolved oxygen located in subsurface silver layers switches over the routes of ethylene oxidation from total oxidation with CO_2 and H_2O production to ethylene epoxidation. The authors suggested that a variation of the electronic structure of atomically adsorbed oxygen is responsible for this selectivity switch.[18] The existence of two different phases of oxygen atomically chemisorbed on the Ag (001) surface has been reported by Rocca *et al.*[19,20] on the basis of the combined photoemission, high-resolution electron energy-loss spectroscopy and x-ray photoelectron diffraction study.

Our previous papers also concluded the formation of several adsorbed oxygen species under *in situ* reaction conditions.[21–25] The identification of various oxygen species was achieved using x-ray photoelectron spectroscopy (XPS) and temperature programmed desorption (TPD). One of these species, which appeared as the result of high-temperature and atmospheric pressure treatment of clean silver with O_2, has been characterized by an O1s binding energy of 529.0 ± 0.2 eV.[21,22] Following traditional TPD nomenclature, this oxygen has been denoted as O_γ because of its higher desorption temperature (~850 K) compared to those of surface adsorbed ($T_{des} \sim 600$ K) and bulk dissolved ($T_{des} \sim 650$–750 K) oxygen, denoted as O_α and O_β, respectively. It has been shown that O_γ is involved in the selective oxidation of methanol to formaldehyde[21,22] and oxidative coupling of methane.[7] The detailed study of O_γ carried out using XPS and ultraviolet photoelectron spectroscopy (UPS), ion scattering spectroscopy, and x-ray-absorption near-edge structure (XANES) spectroscopy[21,22] has shown that this species represents strongly bound atomic oxygen embedded in the outer atomic layer of silver. Such a structure allowed the authors to describe this oxygen as Lewis based, that is, in accordance with its activity in elimination of hydrogen atoms from methanol.

Two other species have been reported in the papers devoted to ethylene epoxidation over silver.[23–25] One of these oxygen species has been characterized by an O1s binding energy of 528.3 ± 0.2 eV and the second one of 530.5 ± 0.2 eV. To clarify their role in ethylene epoxidation, we have monitored the isotopic composition of products during temperature programmed reaction (TPR) of ethylene coadsorbed with the isotopically labeled O_{ads}.[24] The TPR spectroscopy data allowed us to show that the former oxygen is active in a nucleophilic attack of the C-H bond (the first step in total oxidation of ethylene[26]), while the latter is active in an electrophilic addition to the double C=C bond. So, fol-

lowing the paper by Grant and Lambert,[2] these species have been denoted as nucleophilic $[E_b(\mathrm{O1}s)=528.3\ \mathrm{eV}]$ and electrophilic $[E_b(\mathrm{O1}s)=530.5\ \mathrm{eV}]$ oxygen. The same classification will be used in this paper.

While nucleophilic oxygen has been observed in many papers and, as a consequence, has been studied in more detail, the nature of electrophilic oxygen has not been clarified yet. It is evident that elucidation of reasons which cause such considerable variation (up to 2 eV) in O1*s* binding energy should be the first step in this direction. All oxygen species should be characterized using a complementary combination of physical methods, with special attention being paid to the selection of the conditions of formation of the individual species and to their stability during spectroscopic characterization.

In this paper we present the results of a combined photoelectron spectroscopy and x-ray-absorption study for nucleophilic and electrophilic oxygen. We used our previous data[23–25] in order to select the conditions of individual preparation of these oxygen species. As is also shown in this paper, nucleophilic oxygen is prepared by adsorption of pure oxygen, whereas electrophilic oxygen is effectively produced if a clean silver surface is treated with $C_2H_4+O_2$ reaction mixtures. Selective formation of these species allowed us to make the assignment of the observed spectroscopic features more thoroughly.

II. EXPERIMENT

The photoemission part of this investigation was carried out using a VG ESCALAB HP electron spectrometer with the residual pressure $<5\times10^{-10}$ mbar. The differential pumping of the energy analyzer and x-ray tube by diffusion pumps[27,28] makes it possible to measure photoemission spectra *in situ* directly in the analyzer chamber at pressures up to 10^{-4} mbar. Insertion of a special gas cell into the analyzer chamber allows an increase in pressure of *in situ* measurements up to 0.1–0.2 mbar but decreases XPS intensity. The treatment at higher pressures (up to 1 atm) could be realized in the preparation chamber. Subsequent evacuation to UHV followed by transportation of the sample to the analyzer chamber takes about 5 min, and afterwards *ex situ* monitoring of photoemission spectra can be started. The x-ray photoelectron and x-ray-induced Auger electron spectra were taken using Mg $K\alpha$ irradiation ($h\nu=1253.6$ eV) and calibrated against $E_b(\mathrm{Ag}3d_{5/2})=368.2$ eV measured for clean metallic silver. UPS spectra were measured using HeI irradiation ($h\nu=21.2$ eV) and calibrated against the Fermi level. To estimate the oxygen surface coverage $\mathrm{O1}s/\mathrm{Ag}3d_{5/2}$ intensity ratios were recalibrated into fractions of a monolayer (Θ) using our XPS data for the O-(2×1)-Ag(110) low-energy electron-diffraction (LEED) pattern suggesting that the concentration of surface Ag atoms in the polycrystalline silver foil is about 1×10^{15} atoms/cm^2.

The photon-energy-dependent x-ray-absorption spectroscopy measurements were performed at the HE-TGM1 beamline of the Berliner Synchrotron Radiation source, BESSY-I, with an electron-beam energy of 0.8 GeV. A toroidal grating monochromator equipped with two gratings (1100 lines/mm and 1500 lines/mm) was used; it is operated at a resolution of 1.8 eV at the O *K* edge. An x-ray-absorption spectroscopy (XAS) spectrometer attached to BESSY consisted of a double-chamber UHV system with a residual pressure of $<5\times10^{-9}$ mbar. Both the construction of the XAS spectrometer and the procedure of XAS spectra measurement have been described in detail elsewhere.[29] In short, the spectra were collected with the 1100 lines/mm grating in the photon-energy range of 250 eV$\leqslant h\nu\leqslant$1000 eV. C *K*-edge and O *K*-edge spectra have been accumulated with total electron yield detection using an accelerating voltage of +4.5 V. The O *K*-edge spectra were calibrated using an XAS signal of the gas phase oxygen at 530.8 eV recorded at O_2 pressure of 10^{-1} mbar.

The same polycrystalline foil of silver (Goodfellow, 99.95%) was used as a sample for XAS and photoemission measurements. For both types of experiments, the sample was cleaned by the standard high-vacuum cycle: Ar^+ sputtering, annealing in 10 mbar of O_2 at 570 K, and flashing up to 800 K in UHV. More than ten repetitions of this procedure were necessary to exclude observation of any impurities in the XPS spectra and to obtain invariable XAS spectra of C *K*-edge and O *K*-edge. For XAS measurements the specimen were mounted to an aluminum nitride plate (electrically insulating but thermally conducting) with a thickness of $\sim$1.5 mm and an area of 25×25 mm^2 (Hoechst AG) by two nickel clips. The aluminum nitride plate was attached to a boron nitride plate ($\sim$4 mm, Goodfellow). A resistively heated graphite plate covered with boron nitride and mounted between the AlN and BN plates was used to heat the sample. The sample temperature was measured with an alumel-chromel thermocouple attached directly at the back of the sample. In the case of XPS experiments, the sample was fixed on a standard holder, which contained a resistive heating element and an alumel-chromel thermocouple for the temperature control.

III. RESULTS

To measure individual spectral characteristics of the oxygen species, two different sets of experiments were carried out. In the first set, photoelectron and x-ray-absorption spectra were monitored *in situ* at $P(O_2)=10^{-4}$ mbar and $T=470$ K. The experiments of the second set included the pretreatment of a clean silver with $C_2H_4(2.5\%)+O_2$ reaction mixture for 2 hr at $P=1$ mbar and $T=470$ K followed by evacuation and *ex situ* monitoring of the corresponding spectra. These conditions have been selected on the basis of literature data[1–3,10–14] and our own preliminary experiments.[17,23–25] The adsorption of pure O_2 on a clean silver surface effectively produces nucleophilic oxygen, whereas electrophilic oxygen accumulates in measurable amounts during the treatment of silver with a mixture of O_2 with ethylene at $P\geqslant1$ mbar.

Special measures were also taken to avoid the appearance of other oxygen-containing species, the spectral characteristics of which could mask those of the adsorbed oxygen. To avoid the modification of subsurface silver layers by incorporation from the reaction mixture,[25] the lowest possible

pressure (1 mbar) and a small content of ethylene (2.5%) in the reaction mixture were applied for generating the electrophilic oxygen. The temperature of the experiments (470 K) was chosen to provide the stability of the adsorbed oxygen [$T_{des} > 500$ K (Refs. 10–14, and 23–25)] and to prevent the formation of surface carbonates [$T_{decomp} = 420$–450 K (Refs. 11–13)]. It should be also noted that the possibility of *in situ* measurements at $P(O_2) = 10^{-4}$ mbar is of importance since it allowed us to maintain the saturation coverage ($\Theta = 0.5$) of highly active nucleophilic oxygen in the steady-state regime, when its removal due to oxidation processes with ethylene and unavoidable gas phase impurities was compensated by O_2 adsorption from the gas phase.

A. XPS data

Figure 1 presents O1*s* and Ag3*d* core-level spectra from polycrystalline silver recorded during the O_2 adsorption (curve 1) and after the $C_2H_4 + O_2$ reaction mixture treatment (curve 2). The spectra from the clean silver surface are also shown for comparison. One can see that the clean surface is characterized by the complete absence of any intensity in the O1*s* spectrum, indicating that the amount of residual oxygen that has been observed in many previous papers[23,24,30,31] is lower than that of the XPS sensitivity level. The ''clean'' Ag3*d* spectrum exhibits features which can be assigned to the $Ag3d_{5/2}/Ag3d_{3/2}$ doublet (368.2 eV/374.2 eV) originating from spin-orbit splitting, to the $Ag3d_{3/2}$ component (i) excited by the Mg $K\alpha_4$ satellite irradiation line ($\Delta h\nu = 9.8$ eV) and to the $Ag3d_{3/2}$ component (ii) excited by Mg $K\alpha_3$ ($\Delta h\nu = 8.4$ eV), respectively, and to the contribution from a plasmon (iii) characteristic of metallic silver. All these components are easily seen as result of deconvolution of the total Ag3*d* spectrum onto separate components provided that the values of spin-orbital splitting (6.00 eV) and a full width at half maximum [(FWHM) = 1.1 eV] of the lines are fixed. This deconvolution, made using the FITXPS program,[32] is presented in Fig. 1(b).

Oxygen adsorption gives rise to a single O1*s* feature at 528.3 ± 0.1 eV [Fig. 1(a), curve 1]. This binding-energy value has been reported in many papers[12–14,19–25] and indicates the formation of nucleophilic oxygen. Its appearance is accompanied by broadening of Ag3*d* peaks [Fig. 1(b)] due to the appearance of additional components. Note that although all components of the Ag3*d* spectrum appeared as a result of nonmonochromated x-ray irradiation (see the $Ag3d_{5/2}$ spectrum from the clean sample) taken into account for the deconvolution, only those components, which have been excited by the main Mg $K\alpha_{1,2}$ irradiation line, are shown in the figure. The binding-energy splitting and the relative intensities of the oxygen-induced lines allow attributing them to an $Ag3d_{5/2}/Ag3d_{3/2}$ doublet (367.7 eV/373.7 eV) that is lower in binding energy by 0.5 eV compared to metallic silver.

A different O1*s* feature at 530.4 ± 0.1 eV appears when clean silver is treated with the $C_2H_4 + O_2$ reaction mixture [Fig. 1(a), curve 2]. Deconvolution of the corresponding

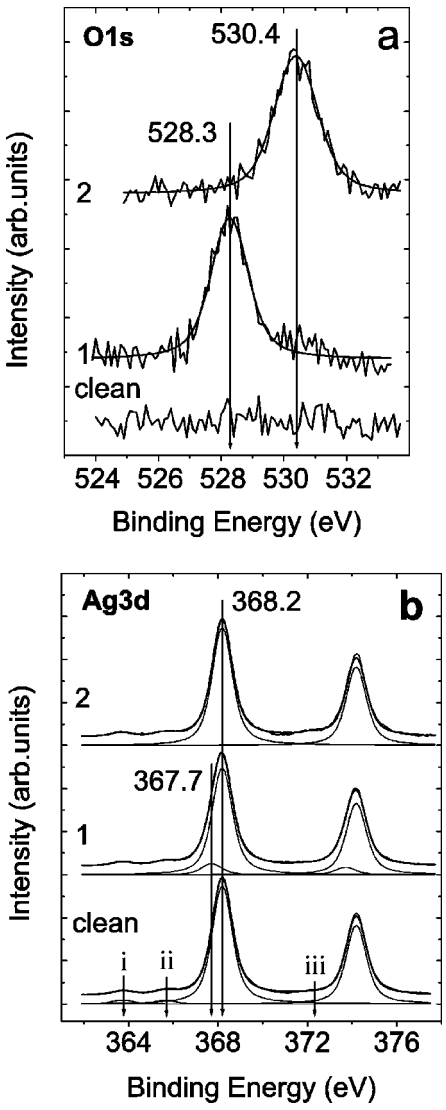

FIG. 1. (a) O1*s* and (b) Ag3*d* core-level spectra from polycrystalline silver foil measured during O_2 adsorption at $P = 10^{-4}$ mbar and $T = 470$ K (curve 1) and after interaction with the $C_2H_4 + O_2$ reaction mixture for 1 h at partial pressures of $P(C_2H_4) = 5 \times 10^{-2}$ mbar and $P(O_2) = 2$ mbar, and $T = 470$ K (curve 2). The spectra from the clean silver are also shown for comparison.

$Ag3d_{5/2}$ spectrum [Fig. 1(b), curve 2] shows that the appearance of this O1*s* line is not accompanied by changes of the ''clean'' Ag3*d* spectrum.

Unfortunately, the binding energy of the new O1*s* line is not so informative as it is in the case of nucleophilic oxygen, since not only adsorbed oxygen, but also surface hydroxyls[33,34] or carbonates[12,13,28] could be responsible for this XPS signal. However, its stability at $T = 470$ K in UHV (conditions of the spectrum monitoring) seems to suggest that surface complexes, other than adsorbed oxygen, can be excluded. Indeed, both OH_{ads} and $CO_{3,ads}$ should desorb at lower temperatures of 360 K and 450 K, respectively. Most probably, the signal arises from the electrophilic oxygen, which is well known to be produced effectively at these reaction conditions.[23–25] The assignment of this O1*s* feature to the adsorbed oxygen, but not to carbonates or hydroxides, is

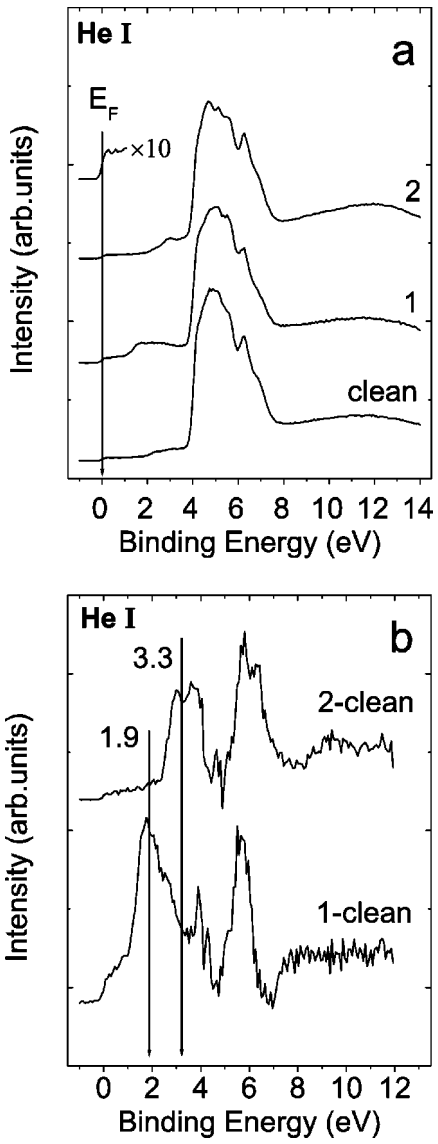

FIG. 2. HeI valence-band spectra from polycrystalline silver foil measured during O_2 adsorption at $P=10^{-4}$ mbar and $T=470$ K (curve 1) and after interaction with the $C_2H_4+O_2$ reaction mixture for 1 hr at partial pressures of $P(C_2H_4)=5\times10^{-2}$ mbar and $P(O_2)=2$ mbar, and $T=470$ K (curve 2). Spectra are presented (a) as is and (b) after subtraction of the spectrum from the clean surface, also shown for comparison.

also confirmed by C1*s* data showing the absence of the carbonate-derived feature at ~287.5 eV and by UPS data (see below).

The data of this chapter demonstrate that the conditions chosen for the oxygen species formation and the *in situ* spectra monitoring provide individual formation and detection of nucleophilic and electrophilic oxygen. Indeed, the FWHM of the features in the O1*s* spectra [Fig. 1(a)] are rather narrow (1.2–1.4 eV) and the ratio of their integrated intensity to the Ag3*d* signal corresponds to a coverage of half a monolayer.

B. UPS data

Figure 2(a) shows HeI ($h\nu=21.22$ eV) ultraviolet photoelectron spectra from the clean silver surface and from silver surfaces covered by nucleophilic (curve 1) and electrophilic (curve 2) oxygen, as well as the corresponding difference spectra [Fig. 2(b)]. One can see that the ''clean'' UPS spectrum consists of the silver peaks at 4–7 eV below the Fermi level originating from the Ag4*d* band emission,[21,28,35–38] and of a threshold near the Fermi level originating mainly from the Ag5*s* emission. The additional intensity in the range of binding energies from 2 to 4 eV can be assigned to satellites of the Ag4*d* lines due to HeI β ($h\nu=23.08$ eV) radiation.[38] This signal, since it is not an indicator of impurities on the clean sample, was also observed earlier for clean Ag(111) Ref. 21 and Ag(110).[36–38]

The adsorption of pure O_2 or of the reaction mixture modifies the ''clean'' UPS spectrum. The high intensity of the Ag4*d* emission obscures small adsorbate-induced signals. Difference spectra corrected for the adsorbate screening are presented in Fig. 2(b). One can see that additional features appear in two ranges of binding energies: 2–4 eV and 5–6 eV. The features located above the Ag4*d* band have been reported in many previous papers[19–21,35–38] and were assigned to O2*p*-derived states. They exhibit a considerable difference in the binding-energy values for nucleophilic (~1.9 eV) and electrophilic (~3.3 eV) oxygen. The assignment of features located inside the Ag4*d* band and even their observation are still under discussion.[35–38] However, individual formation of the oxygen species and accurate preparation of the difference spectra unambiguously show their presence in the valence-band spectra [Fig. 2(b)]. In contrast to the signals above the Ag4*d* bands, these features exhibit much closer binding energies for nucleophilic (~5.7 eV) and electrophilic (~6.0 eV) species. It should be also noted that the spectral regions for hydroxide and carbonate photoemission [8.2/11.0 eV (Refs. 36 and 37) and 8.5 eV,[35] respectively] are free from any features.

C. Auger data

Figure 3 shows Mg $K\alpha$-excited OKLL spectra measured for nucleophilic (curves 1) and electrophilic (curves 2) oxygen. Our choice of Auger spectroscopy, which nowadays is rarely used to study adlayers, is explained by its ability to obtain additional information about the electronic structure of the oxygen species. First, the position of the main Auger line is used to estimate the contribution of the relaxation effect in the observed shift of binding energies. This approach suggested by Wagner[39,40] was later modified by Hohlneicher *et al.*[41] Second, as shown earlier for binary oxides,[42,43] the separation and relative intensities of the $OKL_{23}L_{23}$ and $OKL_{23}L_1$ lines are indicators of the ionicity of the oxygen-metal interaction. A quantitative correlation has been established between the parameters of the OKLL Auger spectra and the formal charge on the oxygen.[44] Finally, it is well known that x-ray-induced Auger spectra are very sensitive to the local electronic structure of oxygen.[45–47]

The Auger spectra were recorded in two modes: OKLL Auger survey spectra with medium resolution and high sensitivity [Fig. 3(a)] and high-resolution spectra of the main $OKL_{23}L_{23}$ line [Fig. 3(b)]. Since the fine structure of the

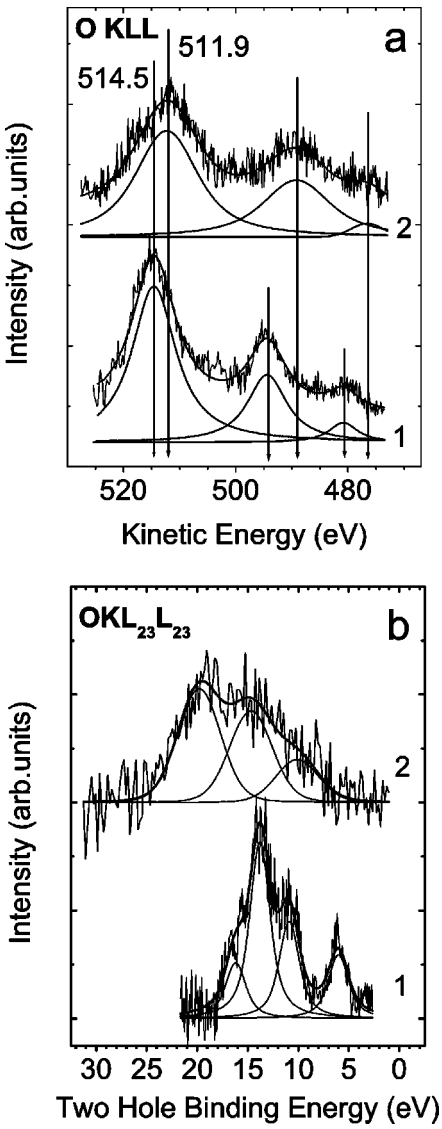

FIG. 3. (a) Auger survey OKLL spectra and (b) fine structures of the main $OKL_{23}L_{23}$ line from polycrystalline silver foil measured during O_2 adsorption at $P=10^{-4}$ mbar and $T=470$ K (curves 1) and after interaction with the $C_2H_4+O_2$ reaction mixture for 1 hr at partial pressures of $P(C_2H_4)=5\times10^{-2}$ mbar and $P(O_2)=2$ mbar, and $T=470$ K (curves 2).

$OKL_{23}L_{23}$ spectra reflects the valence-band structure, the kinetic-energy scale in Fig. 3(b) has been translated into a two-hole binding-energy scale by subtracting the corresponding O1*s* core-hole binding energy.[47] One can see that the kinetic-energy values of the main $OKL_{23}L_{23}$ line and the splitting between the $OKL_{23}L_{23}$ and $OKL_{23}L_1$ lines are quite different for nucleophilic and electrophilic oxygen species [Fig. 3(a)]. The measurement of the dominant $OKL_{23}L_{23}$ line with high resolution exhibits the fine structure of the spectra [Fig. 3(b)], revealing significant differences in the structure for nucleophilic and electrophilic oxygen. The spectrum of the former species can be easily approximated by a series of rather narrow lines, whereas the shape of the second spectrum indicates much wider individual contributions, as suggested by the deconvolution data. Except for an apparently lower FWHM of the lines, the spectrum of nucleophilic oxygen exhibits one additional component located closer to the Fermi level ($E_b=6$ eV).

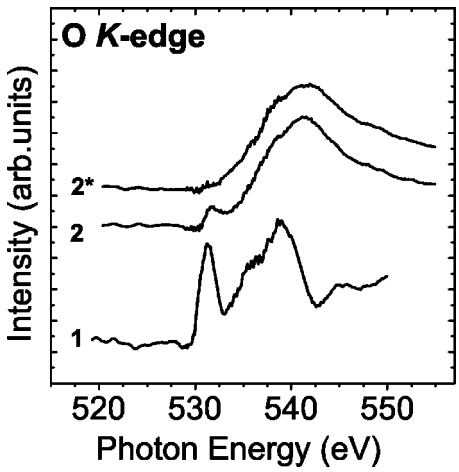

FIG. 4. O *K*-edge spectra from polycrystalline silver foil measured during O_2 adsorption at $P=10^{-4}$ mbar and $T=470$ K (curve 1) and after interaction with the $C_2H_4+O_2$ reaction mixture for 1 hr at partial pressures of $P(C_2H_4)=5\times10^{-2}$ mbar and $P(O_2)=2$ mbar, and $T=470$ K (curve 2). In the latter case, the O *K*-edge spectrum has been recorded also after heating the surface up to 670 K in UHV (curve 2*).

D. XANES data

Similar to all the photoemission spectra, O *K*-edge absorption spectra from the silver polycrystalline foil were recorded during O_2 adsorption and after treatment with the $C_2H_4+O_2$ reaction mixture at $T=470$ K. To observe the XAS signals from adsorbed oxygen, the raw spectra were divided by the spectrum of a clean silver surface recorded under the same conditions. The corresponding difference spectra are shown in Fig. 4. In spite of application of a different UHV system (see Sec. II), the same sample and identical preparation conditions allow us to assign the observed XAS spectra to nucleophilic (Fig. 4, curve 1) and electrophilic (Fig. 4, curves 2 and 2*) oxygen.

One can see that both the XAS spectra exhibit strong structures up to 20 eV above the threshold, but their shapes are quite different. Nucleophilic oxygen gives rise to two signals at photon energies of ~531 and ~539 eV, whereas the electrophilic oxygen is characterized by one broad feature at 541 eV. The small signal at 531 eV observed after treatment of silver with the reaction mixture (Fig. 4, curve 2) seems to arise from the presence of a small amount of nucleophilic oxygen. This suggestion is based on removal of this signal after heating the treated surface up to 570 K, which is in good agreement with the desorption temperature of nucleophilic oxygen.[8–17] The absence of the corresponding signal with E_b (O1*s*)=528.2 eV (Refs. 12–14 and 23–25) in the XPS spectrum [Fig. 1(a), curve 1] can be explained by quick removal of this highly active oxygen via reaction with the hydrocarbon background due to diffusion pumping of the electron spectrometer. In contrast to the XPS spectrometer, the UHV chambers of the XAS spectrometer

are equipped with turbomolecular pumps, which provide hydrocarbon-free residual gases. The assignment of the remaining XAS feature at ~541 eV to the electrophilic oxygen is confirmed by its disappearance when the sample is heated up to 770 K. This temperature coincides with the desorption temperature of electrophilic oxygen.[24,25]

XAS of electrophilic oxygen (Fig. 4, curve 2*) provides unambiguous evidence of its atomic origin. One can see that the photon energy range of 530–535 eV typical of π^* and σ^* transitions of molecular oxygen[48,49] is absolutely free from any signals (Fig. 4, curve 2*). A detailed discussion of this and other arguments in the favor of the atomic nature of this oxygen species can be found in our previous papers.[25,50] According to the literature,[22,51,52] the signals in the photon energy region of 5–10 eV above the threshold in the O *K*-edge spectrum of atomic oxygen originate from a transition of O1*s* electrons to the oxygen 2*p* level, depleted due to hybridization with metal 5*sp* states. A pronounced feature near threshold (~531 eV) in the XAS spectrum of nucleophilic oxygen, which is generally recognized to be of the atomic species, arises from the hybridization of oxygen 2*p* orbitals with silver 4*d* character.[22,51,52]

IV. DISCUSSION

The set of photoelectron spectroscopy and x-ray-absorption data presented in Figs. 1–4 indicates considerable differences in spectral characteristics of nucleophilic and electrophilic oxygen species. It is evident that a detailed analysis of the spectral information for each species and its comparison with literature data are necessary to understand which peculiarities of silver-oxygen bonding are responsible for these differences.

A. Nucleophilic oxygen

The O1*s* feature at 528.3 ± 0.2 eV has been observed many times when bulk silver samples with various silver surfaces was exposed to pure O_2 at temperatures above 300 K: Ag(110),[12,13] Ag(111),[14,17] and Ag(001) (Refs. 19 and 20) single crystals, silver foils;[28,53] and films.[54] As a consequence, the nature of oxygen characterized by this O1*s* feature has been extensively studied by various physical methods.[8–17,33–38] It has been shown that regardless of the surface structures, the desorption temperature of this O_{ads} is approximately constant. The desorption feature together with a pronounced increase in the work function [up to 0.8 eV at $\Theta = 0.5$ (Refs. 8–14)], allowed the authors of Refs. 8–17, and 33–38 to describe this species as atomically adsorbed oxidelike oxygen. It has been concluded that the oxidic nature of this species would account for its activity in the nucleophilic attack of a C-H bond in ethylene.[26] This prompted Grant and Lambert to introduce the term ''nucleophilic oxygen.''[2]

A considerable charge transfer from silver to oxygen atoms in the nucleophilic state is also confirmed by the appearance of an ionic component at 367.6 eV in the Ag3$d_{5/2}$ spectrum [Fig. 1(b), curve 1], with its intensity proportional to the surface abundance of nucleophilic oxygen. In the whole range of the coverage (up to half a monolayer), the ratio of the O1*s* signal at 528.3 eV to this Ag3*d* component was close to 0.5. The negative shift of the Ag3$d_{5/2}$ binding energy for silver oxides with respect to metallic silver (368.2 eV) is well known[47,55,56] and testifies to the formation of positively charged silver ions. The reasons for this unusual shift, reported also for a number of other elements [Cd, Cs, Rb, Ba (Refs. 55 and 56)], originate from the adverse contribution to the negative shift from ground-state charge distribution and from final-state relaxation processes different for metal and oxide binding states due to different core-hole screening abilities.

Studies of this oxidic oxygen carried out by structural sensitive methods such as LEED or scanning-tunneling microscopy (STM) (Refs. 9–14, 36–38, 57, and 58) have shown that oxygen atoms in the nucleophilic state agglomerate to some ordered surface structures. Thus, if an Ag(110) surface is dosed with O_2 at $T \geqslant 300$ K, oxygen atoms cause the formation of one-dimensional oxygen-silver chains. Their density varies with oxygen coverage, providing the observation of a series of LEED patterns from (7×1) to (2×1) at $\Theta = 0.5$.[9–11,36–38] Island formation was concluded by Campbell for O_{nucl} on Ag(111) on the basis of the fact that the $p(4\times4)$ LEED pattern was observed even with submonolayer oxygen coverage.[14] The geometry of these islands was observed by STM.[58] The ordered structures may be described structurally as a phase of a surface Ag_2O oxide. The invariable intrinsic desorption temperature for different silver samples, as well as the small width of the TPD spectrum of nucleophilic oxygen (~30–50 K),[10–13,17,25] fit well with the assignment to a homogeneous surface oxide.

This conclusion makes it possible to use the literature data for bulk silver(I) oxide to discuss the peculiarities of the oxygen-silver interaction of nucleophilic O_{ads}. Indeed, the valence-band and Auger spectra of bulk Ag_2O (Refs. 21 and 47) are quite similar to those of nucleophilic oxygen reported in this work. As in our case [Fig. 2(a), curve 1], the UPS spectrum of silver oxide consists of two features; at 2–4 eV and at 5–6 eV, with the ratio of their intensity dependent on the irradiation used. Taking into account the known energy dependence of the photoionization cross sections of Ag4*d* and O2*p* levels, the authors identified these regions to contain primarily O2*p* and Ag4*d* spectral weight, respectively. Such interpretation is in line with both our [Fig. 2(a)] and other literature UPS data.[35–38] The intense signal in the binding-energy range of 4–7 eV from the clean surface is assigned to photoelectron emission from silver 4*d* states, whereas the features above the 4*d* band appeared as a result of O_2 adsorption—to the adsorbed oxygen.

More ambiguous is the assignment for the oxygen-induced emission inside the Ag4*d* band (5–7 eV), where the emission from the O2*p* levels of adsorbed oxygen is quite possible. Such a peak is commonly observed for many metals,[59,60] but for Ag it is masked by the intense 4*d* emission. As a consequence, the reports about its observation[35–37] are rather contradictory. The difference spectra used in this paper allow to unambiguously observe a feature in this range of binding energies [Fig. 2(b), curve 1]. According to Feydt *et al.*[59] who studied atomic oxygen on W(110), the feature at

$\sim$5.7 eV can be assigned to the atomic O2p orbital, while the feature above the Ag4d band should be attributed to emission from the silver-oxygen hybridized state.

The nature of the valence band as a combination of quasiatomic and hybridized states is very consistent with the fine structure of the $OKL_{23}L_{23}$ spectrum from nucleophilic oxygen [Fig. 3(b), curves 1]. The comparison of these data with spectra of atoms with a filled 2p shell, such as Ne or Mg,[46,61] allows us to assign the features at 10.9, 13.8, and 16.2 eV to different two-hole final states denoted as ^{3}P, ^{1}D, and ^{1}S, respectively, appearing as a result of the spin-orbit coupling. The additional line at $\sim$6 eV can be attributed to a final state having one hole on oxygen and another on silver.[45,46] It is obvious that the probability of such a process and, hence, the intensity of the related peak, will be increased with the extent of hybridization of oxygen orbitals with the silver d band. The same interpretation for this low binding-energy feature has been used in the literature,[47] where the experimental $OKL_{23}L_{23}$ spectrum of Ag_2O was compared with the calculated local O2p^4 density of states (two-hole approximation). Unfortunately, the relevant integrated Auger data for nucleophilic oxygen are not available, since only electron-excited Auger electron spectroscopy has been used in most papers to characterize it.[8,13,14,36]

We conclude that all photoelectron (O1s core level, valence band, Auger $OKL_{23}L_{23}$) spectra of nucleophilic oxygen are very close to the data characteristic of bulk silver(I) oxide. The same situation is observed for the XANES data, which are presented in Fig. 5(a). The comparison of the O K-edge spectrum of nucleophilic oxygen with the corresponding spectrum of bulk Ag_2O reveals their close similarity. Both spectra are characterized by two strong signals at different photon energies: near the threshold $\sim$531 eV and 3–20 eV above the threshold. The strong signals in the O K-edge spectra indicate that in both cases the oxygen-silver interaction is characterized by a high degree of covalency. Indeed, in a purely ionic model, oxygen would exist in the configuration O $1s^2 2s^2 2p^6$, and the $1s \rightarrow 2p$ channel (O K edge) would be closed for XAS.[62] Covalency reduces the number of filled states with O2p character so that O2p-derived orbitals become partly unoccupied. This provides the appearance of signals in the O K-edge XAS, with their intensity being related to the degree of covalency of the O-Ag interaction. The other interesting conclusion arising from the XAS data is the hybridization of O2p orbitals with Ag4d levels. The XAS signals near the threshold are assigned to O2p hybridization with 4d levels of silver.[9,51,52] It should be noted that the participation of Ag4d electrons in bonding of nucleophilic oxygen with the silver surface is in accordance with the photoelectron spectroscopy data, namely, with the appearance of the ionic component in the Ag3d spectrum [Fig. 1(b), curve 1] and with the separate feature at $\sim$6 eV in the $OKL_{23}L_{23}$ Auger spectra [Fig. 3(b), curves 1].

Unambiguous evidence of participation of Ag4d electrons in the formation of the oxygen-silver bonds in bulk Ag_2O can be found in papers by Behrens *et al.* who have monitored Ag L_3-edge XAS data for a number of silver compounds and

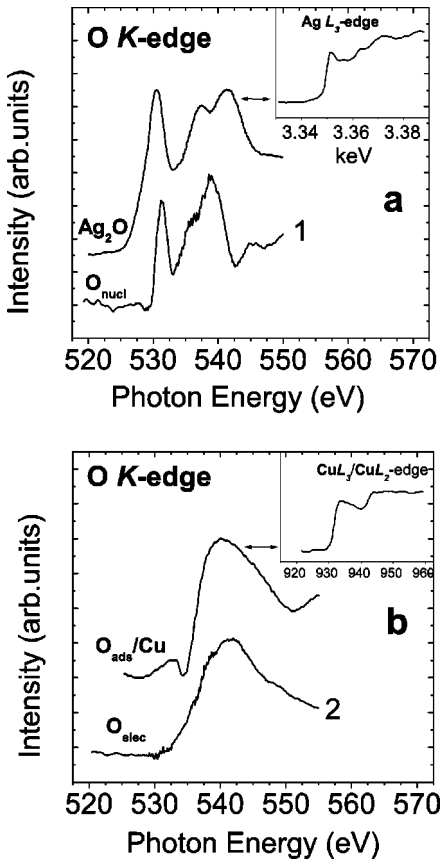

FIG. 5. (a) and (b) Comparison of the O K-edge spectra of the nucleophilic (curve 1) and electrophilic (curve 2) oxygen with the spectra from (a) bulk silver(I) oxide and from (b) polycrystalline copper foil during the conversion of methanol at catalyst temperature of 600 K. For the reference cases (bulk Ag_2O and O_{sub}/Cu) the corresponding Me L edges are also shown as insets.

compared them with the spectrum of metallic silver.[63,64] The corresponding spectrum from bulk Ag_2O taken from Ref. 64 is shown in the inset of Fig. 5(a). One can see that this spectrum is characterized by absorption at about 3.35 keV. In previous experimental[63] and theoretical[65] investigations, this feature has been attributed to dipole-allowed $2p_{3/2} \rightarrow 4d$ transitions. The absence of this feature for metallic silver indicates that all Ag4d states are occupied in this case. Its appearance for silver(I) oxide has been used by the authors to conclude that Ag4d states are partly depleted. This observation is in contradiction with the rule about nonparticipating filled subshells (such as the formal $4d^{10}$ configuration of Ag^+) in chemical bonding. To explain this contradiction, the authors have suggested that the formation of chemical bonds between oxygen and silver atoms results in a partial transfer of electron density from the Ag4d to the Ag5s orbital.[63,64] In this case the electronic configuration of the silver ions can be described as $4d^{10-\delta}5s^{\delta}$. Note that this configuration is in good agreement with the structure of the O K-edge XAS spectra both for nucleophilic oxygen and for bulk Ag_2O [Fig. 5(a)].

Thus, according to all presented data nucleophilic oxygen can be described as oxygen incorporated in the structure of

TABLE I. Experimental energy shifts (eV) ΔE_b (O1s), ΔE_b (O2p), and $\Delta E_A(\mathrm{OKL_{23}L_{23}})$, and initial $\Delta\epsilon$ (O1s) and final ΔR state contributions in the variation of O1s binding energy for different oxygen species on silver.

Type of O_{ads}	O1s	O2p	OKLL	Δ (O1s)	Δ (O2p)	Δ (OKLL)	2Δ(O2p)-Δ(O1s)	ΔR	$\Delta\epsilon$ (O1s)
Nucleophilic	528.3	1.9	514.5	0	0	0	0	0	0
Electrophilic	530.4	3.3	511.9	2.1	1.4	−2.6	0.7	−0.9	−1.2
Ag_2O	528.9	2	513.9	0.6	0.1	−0.6	−0.4	−0.5	−0.1

surface silver(I) oxide. The oxidic nature of the Ag_2O surface oxide determines the activity of this oxygen in the nucleophilic breaking of C-H bonds, which is the first step towards the total oxidation of ethylene. At the same time, the existence of Ag^+ counter ions has a positive influence on the selective oxidation since they provide the formation of π complexes of ethylene, which are probable intermediates in ethylene epoxidation.[66] It should be noted that the description of the silver-oxygen bond in this case as purely ionic is not completely correct, since it is in disagreement with the XANES data. The latter demonstrate both the O2p and Ag4d orbitals to be partly unfilled due to hybridization. This suggests a considerable degree of covalency in the oxygen-silver bond.

B. Electrophilic oxygen

The discussion on the nature of the electrophilic oxygen should start with answering the question asked in the Introduction, i.e., what peculiarities of oxygen-silver bonding determine such a considerable increase in its O1s binding energy as compared to the corresponding value for nucleophilic oxygen [Fig. 1(a)]. It is pointed out that the reasoning is based on an atomic model, since the molecular nature of electrophilic oxygen as one of the most probable reasons of its high binding-energy value can be fully ruled out by our previous XANES experiments.[50]

For the discussion of the differences in valence state of electrophilic oxygen compared to the oxidelike nucleophilic one, it is useful to estimate the contribution of the relaxation effect to the variation in binding energy.[56] We chose the approach that suggests that the relaxation shifts binding energies of the inner and outer shells by different values. To take this effect into account, Hohlneicher *et al.*[41] proposed the following, instead of the well-known Wagner's equation:[39,40]

$$\Delta\alpha = \Delta[E_b + E_A] = 2\Delta R, \tag{1}$$

where $\Delta\alpha$ is the variation of the modified Auger parameter equal to the sum of the kinetic energy of the most prominent Auger line and the binding energy of the XPS line, to use the following relation:

$$\Delta\beta = \Delta[2E_b(i) - E_b(k) + E_A(kii)] = 2\Delta R. \tag{2}$$

The modified equation reflects the fact that the variation of binding energy of the outer shell (i) contributes to Auger transition together with the core level (k).

O1s [Fig. 1(a)] and O2p [Fig. 2(b)] binding energies and kinetic energies for the $\mathrm{OKL_{23}L_{23}}$ Auger transition [Fig. 3(a)] are collected in Table I together with the calculated shifts of energies determined with respect to characteristics of nucleophilic oxygen. From the measured energy shifts we calculated ΔR and, finally, the ''true'' variation of orbital energy ($\Delta\epsilon$) according to

$$\Delta\epsilon = -[\Delta E_b + \Delta R]. \tag{3}$$

Table I further contains the parameters for bulk silver(I) oxide. The original values of the Ag_2O energies have been taken from Ref. 47.

One can see that the shift of the O1s binding energy for bulk Ag_2O compared to the value for nucleophilic oxygen (0.6 eV) is determined essentially by the relaxation contribution. The subtraction of the relaxation shift from the total variation of O1s binding energy leads to a very small difference (0.1 eV) in orbital energy of nucleophilic oxygen and oxygen in the structure of bulk Ag_2O. This is a strong additional confirmation of the chemical similarity of the oxygen-silver interaction in two two-dimensional and three-dimensional silver oxides. The more effective compensation of the core hole that remained after emission of an O1s electron from nucleophilic oxygen can be explained by the direct contact of a surface oxide with metallic silver and enhancing extra-atomic relaxation due to the electron transfer from the electron gas of the underlying metal. The contribution of the final-state relaxation effect to the variation of the O1s binding energy is also rather considerable for electrophilic oxygen (Table I). Approximately half of the shift of E_b (O1s) between O_{elec} and O_{nucl} originates from the relaxation and only half of the shift is determined by the initial-state effect, i.e., by the changes in the electron configuration of oxygen atoms. The increase in the orbital energy for a negatively charged ion means a decrease in the charge[56] on electrophilic oxygen.

Additional confirmation of a considerable decrease of the charge on the electrophilic oxygen originates from the analysis of the Auger spectra. The advantage of this approach, dealing with the structure of the whole OKLL Auger group [Fig. 3(a)], consists of an insignificant contribution of the relaxation effect to the experimental data monitored in the same experiment. Wagner *et al.*[43] emphasized that the spacing between the $\mathrm{OKL_{23}L_1}$ structure and the dominant $\mathrm{OKL_{23}L_{23}}$ Auger structure varies between about 20 eV and 25 eV for a number of oxides, hydroxides, salts, etc. The authors have shown that the increase in the line separation

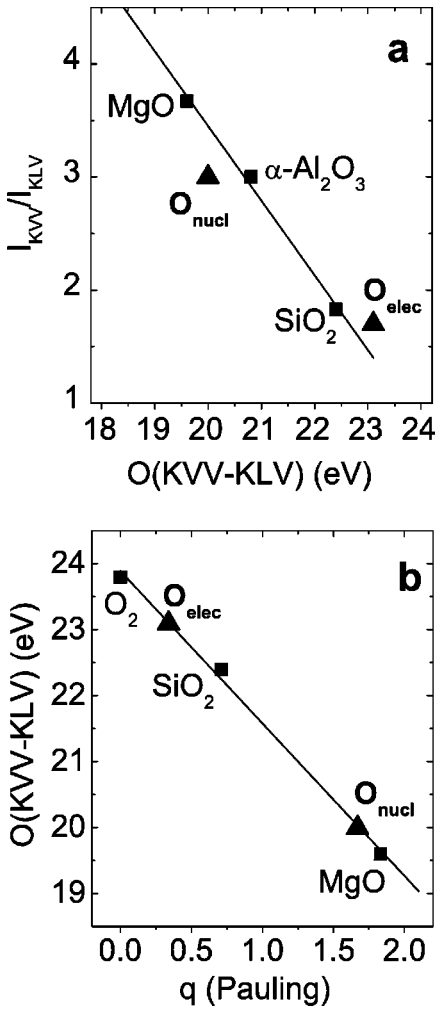

FIG. 6. Relationships of the spacing of the $OKL_{23}L_1$ and $OKL_{23}L_{23}$ Auger lines with their (a) relative intensities and (b) atomic charge on the oxygen calculated using Pauling's electronegativity scale for the oxygen species on the silver surface [Fig. 3(b)] and for a number of binary oxides (Ref. 67).

arises from a decrease in the ionic character of the oxygen-metal bond. At the same time, Weiâmann[42] has shown that intensity ratios of the $OKL_{23}L_{23}$ and OKL_1L_1 Auger lines are correlated quantitatively with the atomic charges on oxygen calculated on the basis of Pauling's scale of electronegativity. A detailed analysis of both parameters of the OKLL Auger group can be found in the paper by Ascarelli and Moretti,[44] who revealed a good correlation between the separation of the $OKL_{23}L_{23}/OKL_{23}L_1$ oxygen lines and their relative intensities. This correlation together with the points for nucleophilic and electrophilic oxygen are shown in Fig. 6(a). One can see that our experimental data are in good agreement with the published correlation, indicating a significant variation of the ionicity in the silver-oxygen interaction for the oxygen species studied. To make quantitative estimation of this variation, we juxtaposed the $E_{kin}(OKL_{23}L_{23}) - E_{kin}(OKL_{23}L_1)$ values for nucleophilic and electrophilic oxygen [Fig. 5(b)] with the dependence taken from Ref. 44. In this dependence, the Auger line separation is connected with the atomic charge on oxygen calculated using Pauling's electronegativity scale.[67] One can see that, in good agreement with the O1*s* orbital energy variation (Table I), the atomic charge on the electrophilic oxygen is by ~1.3 units lower than that on nucleophilic O_{ads}. The deviation of the oxygen charge (~1.65) in the nucleophilic species from 2 indicates the presence of hole states in the O2*p*-derived bands, as has been also concluded from the XANES data [Figs. 4 and 5(a)].

The decrease in the electron density at oxygen atoms in the electrophilic state should originate from a different bonding of oxygen with the silver surface. This general conclusion is confirmed by XANES data. Indeed, the O *K*-edge XAS data of electrophilic oxygen do not exhibit absorption near the threshold (530–532 eV), which is clearly present for nucleophilic oxygen. This fact indicates that Ag4*d* electrons are not involved in the bonding of electrophilic oxygen with the silver surface. This conclusion is in accordance with the absence both the ionic components in the Ag3*d* spectra [Fig. 1(b), curve 2] and of a low binding-energy peak in the $OKL_{23}L_{23}$ spectrum [Fig. 3(b), curves 2] measured from the Ag surface containing electrophilic oxygen.

A similar O *K*-edge spectrum to that presented here was revealed in recent papers[68,69] devoted to an *in situ* XAS study of the selective oxidation of methanol over copper. The corresponding spectrum recorded at 600 K is presented in Fig. 5(b). On the basis of these data, the formation of a suboxide has been concluded. A good agreement with the O *K*-edge spectrum of electrophilic oxygen indicates the same type of bonding interaction between oxygen and a metal in both cases. The Cu $L_{2,3}$-edge spectrum from the copper surface with the suboxide oxygen [Fig. 5(b), inset] exhibits an absorption step structure, which is typical of a metal. The absence of any ''white'' line indicates that Cu3*d* electrons are hardly involved in the formation of the oxygen-metal bond. Assuming a similar bonding in the oxygen-silver system [Fig. 4(b)], the same conclusion about the participation of only 5*sp* states of silver in the chemical bonding can be made for electrophilic oxygen.

Thus, both photoelectron spectroscopy and x-ray-absorption data allow us to represent electrophilic oxygen as an atomic oxygen adsorbed on the surface of metallic silver with less exchange of electron density between metal and oxygen compared to oxidelike nucleophilic O_{ads}. Only the Ag5*sp* levels participate in the oxygen-silver interaction for electrophilic oxygen. The low electron charge on electrophilic oxygen explains its selectivity towards interaction with the double C=C bond of ethylene, leading to the formation of ethylene oxide.

C. Adsorption models for the oxygen species

A further understanding of the nature of nucleophilic and electrophilic oxygen is impossible without consideration of possible models of adsorption centers that should be followed by theoretical representations of their energetic and spectroscopic characteristics. This will help in the explanation of the uniqueness of silver as a heterogeneous catalyst for ethylene epoxidation.

The similarity of spectroscopic characteristics of nucleophilic oxygen to those of bulk silver(I) oxide suggests a similarity of their structural motives. The lattice structure of bulk Ag_2O consists of Ag-O-Ag fragments with a linear coordination. Namely, linear coordination of the Ag^+ cations has been suggested[64] to be preferable for hybridization of $Ag4d_z^2$ and $5s$ orbitals leading to a valence electron distribution that can be rationalized as $4d^{10-\delta}5s^{\delta}$. A coordination close to linear has been concluded for the (2×1)-O structure on an Ag(110) surface on the basis of STM (Ref. 57) and photoelectron-diffraction[70] data. It should be remembered that the (2×1)-O adlayer exhibits the same photoemission characteristics as nucleophilic oxygen. Taking into account all these arguments, we can conclude that the adsorption complex for the O_{nucl} should exhibit a linear coordination and may be approximated by the structure of added rows, such as in the case of oxygen adsorbed on the Ag(110) single-crystal surfaces. Quantum chemical calculations of energetic characteristics of various oxygen species adsorbed on Ag(110) (Ref. 71) have shown the participation of Ag $4d$ orbitals in oxygen-silver bonding in the case of the (2×1)-O structure.

A more complex situation is observed for electrophilic oxygen. On one hand, being a purely adsorbed species it cannot be related to any bulk silver oxide. On the other hand, all studies, which reported the O1s feature at 530.5 eV, either did not characterize it by structure-sensitive methods or assigned this signal to other species (carbonates, subsurface oxygen, etc.). The first steps in the formation of this oxygen species under controlled conditions were made in our recent paper, in which O_2 adsorption on Ag(111) has been studied using angular-dependent XPS,[17] and in the paper by Rocca *et al.*[19] who used x-ray photoelectron diffraction to study oxygen adsorption on an Ag(001) single crystal. We have shown that the atomically adsorbed oxygen with E_b (O1s) $=530.0$ eV, produced as a result of room-temperature adsorption, is evidently located at the surface. Quantum chemical considerations published in Ref. 72 allow us to attribute this species to oxygen adsorbed in a threefold position above an octahedral void of the silver lattice. It has been shown that this adsorption position is most favorable energetically. When the crystal temperature is raised from 300 K to 420 K, this oxygen incorporates into silver[17] and reconstructs the uppermost silver layer. The reconstruction is accompanied by a shift of the O1s spectrum from 530.0 eV to 528.2 eV. This scheme of the surface transformations has been confirmed in a recent STM investigation.[58] The agreement in the binding energies of the surface-adsorbed oxygen and of electrophilic oxygen suggests the similarity of their local structure. From the quantum chemical investigation,[72] it follows that only Ag5s electrons participate in the oxygen-silver bonding when a threefold hollow site is the location of the adsorbate. This observation is also in line with all experimental data.

However, it should be noted that this picture of the oxygen adsorption sites seems to depend on the structure of the silver surface. Indeed, principally different models of adsorption sites have been proposed by Rocca *et al.*[19,20] for nucleophilic and electrophilic oxygen on the Ag(001) surface. Basing on x-ray photoelectron-diffraction data,[19] the authors attributed the first oxygen moiety (the O1s feature at 528.3 eV) to adatoms in fourfold hollows of a nonreconstructed Ag(001) surface, and the second one (the O1s feature at 530.3 eV) to adatoms on a missing row, reconstructed surface. A detailed analysis of the proposed structures indicates that only in the latter case can the Ag-O chains be revealed. These results indicate that the nature of oxygen-silver bonding might be more complex, and a further comprehensive study of nucleophilic and electrophilic oxygen species on different crystal planes of silver [i.e., Ag(110) vs Ag(001)] is necessary to clarify this problem.

V. SUMMARY

Exposure of clean silver to O_2 at $P=10^{-4}$ mbar and $T=470$ K produces atomically adsorbed oxygen with E_b (O1s) $=528.3$ eV denoted as the nucleophilic species. A stoichiometry of $Ag_{(x=2\pm0.2)}O$ and an ionic component in the Ag3$d_{5/2}$ spectrum at 367.7 eV allow us to conclude the formation of a surface silver(I) oxide that is confirmed by the similarity of its spectral characteristics with those of bulk Ag_2O. The oxidic nature of the oxygen-silver bond explains both its participation in the total oxidation route and the promotion of ethylene adsorption due to formation of π complexes with positively charged silver ions. Despite a considerable charge transfer from silver to oxygen, which is typical of binary metal oxides, the shape of the XAS spectra indicates the significant covalency of the oxygen-silver interaction. This covalency was attributed to hybridization of O2p orbitals not only with a 5s state, but also with formally filled $4d$ levels of silver.

The treatment of clean silver with C_2H_4 (2.5%)$+O_2$ at $P=2$ mbar and $T=470$ K leads to another type of atomic adsorbed oxygen with E_b (O1s) $=530.4$ eV. As shown earlier, this species named electrophilic oxygen is responsible for the epoxidation route. The estimation of the relaxation contribution to the total shift of its O1s spectrum with respect to nucleophilic oxygen species reveals that about half of the shift can be explained by a final-state effect. The remaining shift originates from a change in the orbital energy. The observed shift of the orbital energy to higher values indicates a decrease in the electron density in electrophilic oxygen atoms. The same conclusion follows from the Auger data, which show a higher separation for the $OKL_{23}L_{23}$ and $OKL_{23}L_1$ lines and a lower ratio of their intensities for electrophilic oxygen than the corresponding values for the nucleophilic one. The absence of signals at 530–535 eV photon energy in the O K-edge spectrum of the electrophilic oxygen clearly indicate that Ag$4d$ electrons do not participate in oxygen-silver bonding in this case.

This detailed spectroscopic analysis was possible only due to a high-pressure high-temperature preparation of the oxygen species and *in situ* observation. A clear correlation of electronic structure and catalytic function was derived after the earlier *in situ* study[50] was combined with the present results. The still missing, exact geometric structures of the two catalytically relevant surface species may be a challenge to theoretical studies using the spectral information of the present study as a reference.

ACKNOWLEDGMENTS

This work was supported in part by the Russian Foundation for Basic Research, Grant No. 00-15-99335. The authors would like to thank the BESSY staff for help in carrying out the XAS experiments. V.I.B. gratefully acknowledges the Max-Planck-Gesselschaft for financial support of his visit to FHI and work at BESSY and the Russian Science Support Foundation grant for young and talented scientists.

*Corresponding author. Email address: vib@catalysis.nsk.su

[1] C. T. Campbell and M. T. Paffett, Surf. Sci. **139**, 396 (1984).
[2] R. B. Grant and R. M. Lambert, J. Catal. **92**, 364 (1985).
[3] R. A. van Santen and C. P. M. de Groot, J. Catal. **98**, 530 (1986).
[4] R. A. van Santen and H. P. C. E. Kuipers, Adv. Catal. **35**, 265 (1987).
[5] M. A. Barteu and R. J. Madix, in *The Chemical Physics of Solid Surfaces and Heterogeneous Catalysis*, edited by D. A. King and D. P. Woodruff (Elsevier, Amsterdam, 1982), Vol. 4, Chap. 4.
[6] S. Hawker, C. Mukoid, J. P. S. Badyal, and R. M. Lambert, Surf. Sci. **219**, L615 (1989).
[7] A. J. Nagy, G. Mestl, and R. Schlögl, J. Catal. **188**, 58 (1999).
[8] G. Rovida, F. Pratesi, M. Maglietta, and F. Ferroni, Surf. Sci. **43**, 230 (1974).
[9] G. Rovida and F. Pratesi, Surf. Sci. **52**, 542 (1975).
[10] C. Backx, C. P. M. de Groot, and R. Biloen, Surf. Sci. **104**, 300 (1981).
[11] C. Backx, C. P. M. de Groot, P. Biloen, and W. M. H. Sachtler, Surf. Sci. **128**, 81 (1983).
[12] M. A. Barteau and R. J. Madix, J. Electron Spectrosc. Relat. Phenom. **31**, 101 (1983).
[13] C. T. Campbell and M. T. Paffett, Surf. Sci. **143**, 517 (1984).
[14] C. T. Campbell, Surf. Sci. **157**, 43 (1985).
[15] C. T. Campbell, Surf. Sci. **173**, L641 (1986).
[16] R. B. Grant and R. M. Lambert, Surf. Sci. **146**, 256 (1984).
[17] V. I. Bukhtiyarov, V. V. Kaichev, and I. P. Prosvirin, J. Chem. Phys. **111**, 2169 (1999).
[18] P. J. van den Hoek, E. J. Baerends, and R. A. van Santen, J. Phys. Chem. **93**, 6469 (1989).
[19] M. Rocca, L. Savio, L. Vattuone, U. Burghaus, V. Palomba, N. Novelli, F. Buatier de Mongeot, and U. Valbusa, Phys. Rev. B **61**, 213 (2000).
[20] L. Savio, L. Vattuone, M. Rocca, F. Buatier de Mongeot, G. Comelli, A. Baraldi, S. Lizzit, and G. Paolucci, Surf. Sci. **506**, 213 (2002).
[21] X. Bao, M. Muhler, Th. Shedel-Niedrig, and R. Schlögl, Phys. Rev. B **54**, 2249 (1996).
[22] Th. Shedel-Niedrig, X. Bao, M. Muhler, and R. Schlögl, Ber. Bunsenges. Phys. Chem. **101**, 994 (1997).
[23] V. I. Bukhtiyarov, A. I. Boronin, I. P. Prosvirin, and V. I. Savchenko, J. Catal. **150**, 262 (1994).
[24] V. I. Bukhtiyarov, I. P. Prosvirin, and R. I. Kvon, Surf. Sci. **320**, L47 (1994).
[25] V. I. Bukhtiyarov, V. V. Kaichev, E. A. Podgornov, and I. P. Prosvirin, Catal. Lett. **57**, 233 (1999).
[26] R. A. van Santen, S. Moolhuysen, and W. M. H. Sachtler, J. Catal. **65**, 478 (1980).
[27] R. W. Joyner, M. W. Roberts, and K. Yates, Surf. Sci. **87**, 501 (1979).
[28] A. I. Boronin, V. I. Bukhtiyarov, A. L. Vishnevskii, G. K. Boreskov, and V. I. Savchenko, Surf. Sci. **201**, 195 (1988).
[29] A. Knop-Gericke, M. Hävecker, and Th. Shedel-Niedrig, Nucl. Instrum. Methods Phys. Res. A **406**, 311 (1998).
[30] L. Lefferts, J. G. van Ommen, and J. R. H. Ross, J. Chem. Soc., Faraday Trans. 1 **83**, 161 (1987).
[31] C. Rehren, M. Muhler, X. Bao, R. Schlögl, and G. Ertl, Z. Phys. Chem. (Munich) **11**, 174 (1991).
[32] D. L. Adams and J. N. Andersen, computer code FITXPS, version 1.13 (Institute of Physics and Astronomy, University of Aarhus, Denmark, 2000), ftp://boopic.dfi.aau/dk/pub/fitxps
[33] M. A. Barteau and R. J. Madix, Surf. Sci. **140**, 108 (1984).
[34] A. F. Carley, P. R. Davies, M. W. Roberts, and K. K. Thomas, Surf. Sci. **238**, L467 (1990).
[35] I. E. Wachs and S. R. Kelemen, J. Catal. **71**, 78 (1981).
[36] K. C. Prince and A. M. Bradshaw, Surf. Sci. **126**, 49 (1983).
[37] K. C. Prince, G. Paolucci, and A. M. Bradshaw, Surf. Sci. **175**, 101 (1986).
[38] D. Sekiba, H. Nakamizo, R. Ozawa, Y. Gunji, and H. Fukutani, Surf. Sci. **449**, 111 (2000).
[39] C. D. Wagner, Faraday Discuss. Chem. Soc. **60**, 291 (1975).
[40] C. D. Wagner, J. Electron Spectrosc. Relat. Phenom. **10**, 305 (1977).
[41] G. Hohlneicher, H. Pulm, and H.-J. Freund, J. Electron Spectrosc. Relat. Phenom. **37**, 209 (1985).
[42] R. Weiâmann, Solid State Commun. **31**, 347 (1979).
[43] C. D. Wagner, D. A. Zlatko, and R. H. Raymond, Anal. Chem. **52**, 1445 (1980).
[44] P. Ascarelli and G. Moretti, Surf. Interface Anal. **7**, 8 (1985).
[45] P. H. Citrin, J. E. Rowe, and S. B. Christman, Phys. Rev. B **14**, 2642 (1976).
[46] J. C. Fuggle, E. Umbach, R. Kakoschke, and D. Menzel, J. Electron Spectrosc. Relat. Phenom. **26**, 111 (1982).
[47] L. H. Tjeng, M. B. J. Meinders, J. van Elp, G. A. Sawatzky, and R. L. Johnson, Phys. Rev. B **41**, 3190 (1990).
[48] R. J. Guest, B. Hernnäs, P. Bennich, O. Björneholm, A. Nilsson, R. E. Palmer, and N. Mårtensson, Surf. Sci. **278**, 239 (1992).
[49] J. Pawela-Crew, R. J. Madix, and J. Stöhr, Surf. Sci. **339**, 23 (1995).
[50] V. I. Bukhtiyarov, M. Hävecker, V. V. Kaichev, A. Knop-Gericke, R. W. Mayer, and R. Schlögl, Catal. Lett. **74**, 121 (2001).
[51] F. M. F. de Groot, M. Grioni, J. C. Fuggle, J. Ghijsen, G. A. Sawatzky, and H. Petersen, Phys. Rev. B **40**, 5715 (1989).
[52] J. Purans, A. Kuzmin, Ph. Parent, and C. Laffon, Physica B **259-261**, 1157 (1999).
[53] R. W. Joyner and M. W. Roberts, Chem. Phys. Lett. **60**, 459 (1979).
[54] A. I. Boronin, V. I. Bukhtiyarov, A. L. Vishnevskii, G. K. Boreskov, and V. I. Savchenko, Kinet. Katal. **25**, 1508 (1984).
[55] J. S. Hammond, S. W. Gaarenstroom, and N. Winograd, Anal. Chem. **47**, 2193 (1975).
[56] J. F. Moulder, W. F. Stickle, P. E. Sobol, and K. D. Bomben, *Handbook of X-ray Photoelectron Spectroscopy*, edited by J. Chastain (Perkin-Elmer, Eden Prairie, 1992).

[57] M. Taniguchi, K. Tanaka, T. Hashizume, and T. Sakurai, Surf. Sci. **262**, L123 (1992).
[58] C. I. Carlisle, T. Fujimoto, W. S. Sim, and D. A. King, Surf. Sci. **470**, 15 (2000).
[59] J. Feydt, A. Elbe, H. Engelhard, G. Meister, and A. Goldmann, Surf. Sci. **440**, 213 (1999).
[60] C. Q. Sun and S. Li, Surf. Rev. Lett. **7**, 213 (2000).
[61] H. Körber and W. Mehlhorn, Z. Phys. **191**, 217 (1966).
[62] J. Stöhr, in *NEXAFS Spectroscopy*, Springer Series in Surface Sciences, Vol. 25, edited by R. Gomer (Springer, Heidelberg, 1992).
[63] P. Behrens, Solid State Commun. **81**, 235 (1992).
[64] P. Behrens, S. Aßmann, U. Bilow, C. Linke, and M. Jansen, Z. Anorg. Allg. Chem. **625**, 111 (1999).
[65] M. T. Czyzyk, R. A. de Groot, G. Dalba, P. Fornasini, A. Kisiel, F. Rocca, and E. Burattini, Phys. Rev. B **39**, 9831 (1989).
[66] D. A. Bulushev, E. A. Paukshtis, Y. N. Nogin, and B. S. Balzhinimaev, Appl. Catal., A **123**, 301 (1995).
[67] L. E. Orgel, J. Chem. Soc. **1958**, 4186.
[68] M. Hävecker, A. Knop-Gericke, Th. Shedel-Niedrig, and R. Schlögl, Angew. Chem., Int. Ed. Engl. **37**, 1939 (1998).
[69] M. Hävecker, A. Knop-Gericke, Th. Shedel-Niedrig, and R. Schlögl, Top. Catal. **15**, 27 (2001).
[70] M. Pascal, C. L. A. Lamont, P. Baumgärtel, R. Terborg, J. T. Hoeft, O. Schaff, M. Polcik, A. M. Bradshaw, R. L. Toomes, and D. P. Woodruff, Surf. Sci. **464**, 83 (2000).
[71] I. L. Zilberberg and G. M. Zhidomirov, J. Struct. Chem. **38**, 528 (1997).
[72] I. L. Zilberberg, M. A. Milov, and G. M. Zhidomirov, J. Struct. Chem. **40**, 350 (1999).